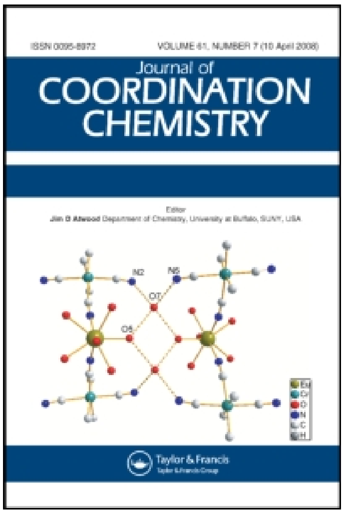

Journal of Coordination Chemistry
Publication details, including instructions for authors and subscription information:
http://www.informaworld.com/smpp/title~content=t713455674

Synthesis and spectroscopic studies of novel mononuclear complexes of cyclic and acyclic Schiff-base derivatives of tridentate and tetradentate coordination with some bivalent transition metal ions

Akila A. Saleh[a]
[a] Department of Chemistry, Faculty of Education, Ain Shams University, Roxy, Cairo, Egypt

To cite this Article Saleh, Akila A.(2005) 'Synthesis and spectroscopic studies of novel mononuclear complexes of cyclic and acyclic Schiff-base derivatives of tridentate and tetradentate coordination with some bivalent transition metal ions', Journal of Coordination Chemistry, 58: 3, 255 — 270

To link to this Article: DOI: 10.1080/00958972512331334199

URL: http://dx.doi.org/10.1080/00958972512331334199

Journal of Coordination Chemistry
Vol. 58, No. 3, 15 February 2005, 255–270

Taylor & Francis
Taylor & Francis Group

Synthesis and spectroscopic studies of novel mononuclear complexes of cyclic and acyclic Schiff-base derivatives of tridentate and tetradentate coordination with some bivalent transition metal ions

AKILA A. SALEH*

Department of Chemistry, Faculty of Education, Ain Shams University,
Roxy, Cairo, Egypt

(Received 31 March 2004; in final form 11 November 2004)

Eight novel cyclic and acyclic Schiff-base ligands, L^1 = 6-amino-3-methyl-1-phenyl-4-aza-3-hepten-1-one, L^2 = 3,7-diaza-2,4,8-trimethyl-6-phenylnona-3,7-diene-1,9-diamine, L^3 = 4,7-diaza-3,5,8-trimethyl-1,10-diphenyldeca-3,7-diene-1,10-dione, L^4 = 3,5,10,14-tetramethyl-7,12-diphenyl-1,4,8,11-tetraazacyclotetradeca-4,7,11,14-tetraene, L^5 = 7-amino-3-methyl-1-phenyl-4-aza-3-hepten-1-one, L^6 = 4,8-diaza-5-methyl-7-phenylundeca-4,8-diene-1,11-diamine, L^7 = 4,8-diaza-3,9-dimethyl-1,11-diphenyldideca-1,11-dione and L^8 = 2,12-dimethyl-4,10-diphenyl-1,5,9,13-tetraazacyclohexadeca-1,4,9,12-tetraene, have been prepared and characterized by elemental analysis, IR, ^{1}H NMR and mass spectroscopy. Their corresponding Co(II), Ni(II), Cu(II), Zn(II) and Cd(II) complexes (**1**–**15**) have been prepared by the reaction of the ligand with the metal sulfate or chloride in a 1:1 molar ratio and characterized by elemental analysis, thermogravimetric analysis (TGA), IR, electronic and magnetic susceptibility measurements. Electronic spectra and magnetic susceptibility measurements of the solid complexes indicate an octahedral geometry around Cu(II), Co(II), Ni(II), Zn(II) and Cd(II) and a square-planar geometry around the Ni(II) complexes of L^2 and L^3. The SO_4^{2-} ion is coordinated to the central metal(II) ion as a bidentate ligand through two oxygen atoms in all of the complexes except those with Ni(II). The chloride ion is coordinated to the central Ni(II) ion in complexes of L^1. The conductances of the complexes are very low, indicating their non-electrolytic nature except for the Ni complex of L^2, whose molar conductance of 192.5 $\text{ohm}^{-1}\,\text{mol}^{-1}\,\text{cm}^2$ indicates an ionic character for $[NiL^2]Cl_2$. The antifungal properties of the ligands and their complexes were investigated.

Keywords: Cyclic and acyclic Schiff bases; Mononuclear metal complexes; IR and mass spectroscopy of metal complexes

1. Introduction

Recent years have witnessed a growing interest in cyclic and macrocyclic complexes of transition metals because of their use as diagnostic agents in magnetic resonance

---

*E-mail: abyad400@soficom.com.eg

Journal of Coordination Chemistry
ISSN 0095-8972 print: ISSN 1029-0389 online © 2005 Taylor & Francis Group Ltd
DOI: 10.1080/00958972512331334199

imaging (MRI) [1]. Such complexes are also significant because of their resemblance to natural systems [2,3]. Many transition metal ions in living systems work as enzymes or carriers in a macrocyclic ligand environment; meaningful research in this direction might generate simple models for biologically occurring metaloenzymes [4], and thus help in further understanding biological systems. These ligands are also of theoretical interest as they are capable of furnishing an environment of controlled geometry and ligand field strength [5–10]. Mixed ligand complexes have attracted interest as enzyme mimics [11]. Complexes containing multidentate mixed-donor ligands have also been investigated as catalysts [12]. The present work reports the synthesis of eight new Schiff-base ligands and 15 new Schiff-base complexes [eight Cu(II), two Co(II), one Zn(II) and one Cd(II) sulfato complexes and three Ni(II) complexes].

2. Experimental

The chemicals used were BDH products. The solvents were purified by recommended procedures [13]. The apparatus, physical measurements and analyses are as described previously [14]. Infrared spectra were recorded with a Perkin-Elmer IR spectrophotometer (4000–200 cm^{-1}) using KBr pellets. Melting points of the compounds were determined using the RUMO melting points apparatus, model 3600. ^{1}H NMR spectra of the compounds were recorded using a Varian EM-390 spectrometer at 90 MHz at the Microanalytical Center, Cairo University, Giza, Egypt. Deuterated DMSO was used as a solvent and TMS as internal reference. Spectra were measured from 0 to 14 ppm. Mass spectra of the ligands and some of the metal complexes were recorded on a Hewlett-Packard MS 5988 at the Microanalytical Center, Cairo University. Fragmentation was carried out at 300°C and 70 eV. Magnetic susceptibilities of the complexes were measured by the Gouy method at room temperature using an MKI Johnson Matthey, Alpha products, magnetic susceptibility balance; mercury(II) tetrathiocyanatocobaltate(II) was used as calibrant. Effective magnetic moments were calculated from the expression $\mu_{\text{eff}} = 2.828(\chi_{\text{m}}T)^{1/2}$ BM, where χ_{m} is the molar susceptibility. Diamagnetic corrections were calculated from Pascal's constants. Thermogravimetric analysis (TGA) of the solid complexes was performed using a Schimadzu TGA-50 instrument in the range 0–700°C at a heating rate of 20°C/min under nitrogen. Conductance measurements of 10^{-3} M solutions of the complexes in DMF were carried out on a Corning 441 conductivity meter. Reflectance spectra of the metal complexes were recorded using a Shimadzu UV-visible spectrophotometer model 1601 in the range 190–1100 nm. The solution spectrum of the metal complexes in DMF was recorded on a JASCO UV-visible spectrophotometer model V-550 in the range 200–900 nm. Elemental analyses (C, H, N and S) were carried out by the Microanalytical Center, Cairo University; analyses of the metal followed decomposition of the complexes with concentrated hydrochloric acid. The resultant solutions were diluted with water and filtered to remove the precipitated ligand. The solution was then neutralized with ammonia solution and the metal ions were titrated with EDTA.

2.1. *Synthesis of cyclic and acyclic Schiff-base derivatives*

The cyclic and acyclic imine ligands were prepared according to the method given in the literature [15]. L^1, L^2, L^3 and L^4 are isomers of L^5, L^6, L^7 and L^8, respectively.

2.1.1. L^1 and L^5. Benzoylacetone (1.62 g, 10 mmol) in methanol (100 cm^3) was added slowly to a solution of 1,2- or 1,3-propane diamine (0.74 g, 10 mmol) in methanol (100 cm^3). The pale yellow solution was stirred at room temperature for 8 h, water was removed, the solvent was evaporated *in vacuo*, and the oily residue was recrystallized from MeOH/ether. After refrigeration for several days [15a], white crystals were obtained. L^1, yield 65%, mp 104°C. Calcd: C, 71.5; H, 8.2; N, 12.8. Found: C, 71.8; H, 8.3; N, 12.6. ^1H NMR ($CDCl_3$) δ (ppm), 1.41 (d, 3H, CH_3), 2.00 (s, 3H, CH_3), 2.42 (t, 1H, CH), 3.5 (s, 2H, CH_2), 4.44 (d, 2H, CH_2), 7.44–7.98 (m, 5H, Ph), 5.8 (br, 2H, NH_2). IR (cm^{-1}), ν max (KBr) 3340–3160 (br, NH_2), 1652 (C=O) and 1600 (C=N). L^5, yield 79%, mp 110°C. Calcd: C, 71.5; H, 8.2; N, 12.8. Found: C, 71.8; H, 8.1; N, 13.1. ^1H NMR ($CDCl_3$) δ (ppm), 1.81 (s, 3H, CH_3), 2.10 (m, 2H, CH_2), 2.74 (s, 2H, CH_2), 3.11 (m, 4H, 2 (NCH_2)), 7.43–7.96 (m, 5H, Ph), 5.8 (br, 2H, NH_2). IR (cm^{-1}), ν_{max} (KBr) 3344–3170 (br, NH_2), 1658 (C=O) and 1600 (C=N).

2.1.2. L^2 and L^6. Benzoylacetone (1.62 g, 10 mmol) in methanol (100 cm^3) was added slowly to a solution of 1,2- or 1,3-propanediamine (1.48 g, 20 mmol) in methanol (200 cm^3). The pale yellow solution was stirred at room temperature for 8 h, water was removed, the solvent was evaporated *in vacuo*, and the oily residue was recrystallized from MeOH/ether. After refrigeration for several days [15a], white crystals were obtained. L^2, yield 69%, mp 155°C. Calcd: C, 70.7; H, 9.5; N, 20.4. Found: C, 69.7; H, 9.3; N, 20.6. ^1H NMR ($CDCl_3$) δ (ppm), 1.00 (d, 6H, $2(CH\text{–}C\underline{H}_3)$), 2.05 (s, 3H, CH_3), 2.28 (s, 2H, CH_2), 2.72 (m, 2H, $2(C\underline{H}\text{–}CH_3)$), 2.88 (br, 4H, $2NH_2$), 3.82 (t, 4H, $2(C\underline{H}_2\text{–}NH_2)$), 7.41–7.84 (m, 5H, Ph). IR (cm^{-1}), ν_{max} (KBr) 3440, 3266 (NH_2), 1632, 1623 (C=N). L^6, yield 64%, mp 127°C. Calcd: C, 70.07; H, 9.5; N, 20.4. Found: C, 70.3; H, 9.4; N, 20.2. ^1H NMR ($CDCl_3$) δ (ppm), 1.91 (m, 4H, $2CH_2$), 2.73 (s, 3H, CH_3), 2.88 (s, 2H, CH_2), 3.11 (br, 4H, $2NH_2$), 3.61 (t, 4H, NCH_2), 3.67 (t, 4H, $2NCH_2$), 7.42–7.94 (m, 5H, Ph). IR (cm^{-1}), ν_{max} (KBr) 3420, 3288 (NH_2), 1659, 1625 (C=N).

2.1.3. L^3 and L^7. Benzoylacetone (3.24 g, 20 mmol) in methanol (200 cm^3) was added slowly to a solution of 1,2- or 1,3-propanediamine (0.74g, 10 mmol) in methanol (100 cm^3). The yellow solution was stirred at room temperature for 8 h, water was removed, the solvent was evaporated *in vacuo*, and the oily residue was recrystallized from MeOH/ether. After refrigeration for several days [15a], white crystals were obtained. L^3, yield 66%, mp 120°C. Calcd: C, 76.2; H, 7.2; N, 7.7. Found: C, 76.0; H, 6.9; N, 7.5. ^1H NMR ($CDCl_3$) δ (ppm), 1.31 (d, 3H, CH_3), 2.08 (s, 3H, CH_3), 2.11 (s, 3H, CH_3), 3.52 (d, 2H, CH_2N), 4.02 (m, 1H, CHN), 5.78 (s, 2H, 2(CH=COH)), 7.42–7.87 (m, 10H, 2Ph), 11.50 (br, 2H, 2OH enol). IR (cm^{-1}), ν_{max} (KBr) 1632, 1624 (C=N). L^7, yield 64%, mp 103°C. Calcd: C, 76.2; H, 7.2; N, 7.7. Found: C, 75.8; H, 7.3; N, 7.8. ^1H NMR ($CDCl_3$) δ (ppm), 1.68 (m, 2H, CH_2), 2.08 (s, 6H, $2CH_3$), 3.56 (t, 4H, $2NCH_2$), 5.80 (s, 2H, $2(C\underline{H}{=}COH)$), 7.44–7.96 (m, 10H, 2Ph), 11.36 (br, 2H, 2OH enol). IR (cm^{-1}), ν_{max} (KBr) 1656 (C=N).

2.1.4. L^4 and L^8. Benzoylacetone (3.24 g, 20 mmol) in methanol (200 cm^3) was added slowly to a solution of 1,2- or 1,3-propanediamine (1.48 g, 20 mmol) in methanol (200 cm^3). The yellow solution was stirred at 50°C for 3 h, water was removed, the solvent was evaporated *in vacuo*, and the oily residue was recrystallized from MeOH/ether. After refrigeration for several days [15a], white crystals were obtained. L^4, yield 63%, mp 92°C. Calcd: C, 78.0; H, 8.0; N, 14.0. Found: C, 77.7; H, 8.09; N, 13.7. ^{1}H NMR ($CDCl_3$) δ (ppm), 1.31 (d, 6H, 2(CH–C$\underline{H}_3$)), 2.10 (s, 6H, $2CH_3$), 2.42 (s, 4H, $2CH_2$), 3.49 (d, 4H, $2CH_2$), 4.02 (m, 2H, 2CH), 7.42–7.87 (m, 10H, 2Ph). IR (cm^{-1}), ν_{max} (KBr) 1632, 1622 (C=N). L^8, yield 68%, mp 85°C. Calcd: C, 78.0; H, 8.0; N, 14.0. Found: C, 78.3; H, 7.8; N, 14.3. ^{1}H NMR ($CDCl_3$) δ (ppm), 1.81 (s, 6H, $2CH_3$), 2.56 (m, 4H, $2CH_2$), 3.41 (s, 4H, 2(CH_2–C=N)), 3.58(t, 8H, 4(CH_2–N=)), 7.44–7.85 (m, 10H, 2Ph). IR (cm^{-1}), ν_{max} (KBr) 1655 (C=N). Mass spectra showed that the parent peak of each compound corresponded to its molecular weight (*m*/*e*).

By adjusting the experimental conditions, different ligands were obtained (figure 1). Ligands L^1 and L^5, and L^3 and L^7, undergo keto–enol tautomerism leading to the formation of enolic OH groups.

The Schiff-base ligands L^1–L^8 prepared are: L^1 = 6-amino-3-methyl-1-phenyl-4-aza-3-hepten-1-one; L^2 = 3,7-diaza-2, 4,8-trimethyl-6-phenylnona-3,7-diene-1,9-diamine; L^3 = 4,7-diaza-3,5,8-trimethyl-1,10-diphenyldeca-3,7-diene-1,10-dione; L^4 = 3,5,10,14-tetramethyl-7,12-diphenyl-1,4,8,11-tetraazacyclotetradeca-4,7,11,14-tetraene; L^5 = 7-amino-3-methyl-1-phenyl-4-aza-3-hepten-1-one; L^6 = 4,8-diaza-5-methyl-7-phenyl undeca-4,8-diene-1,11-diamine; L^7 = 4,8-diaza-3,9-dimethyl-1,11-diphenyl dideca-1,11-diamine; and L^8 = 2,12-dimethyl-4,10-diphenyl-1,5,9,13-tetraazacyclohexadeca-1,4,9,12-tetraene.

2.2. *Synthesis of Schiff-base complexes*

Complexes ML were prepared by the reaction of ligands with metal sulfate or chloride in a 1 : 1 molar ratio.

To a solution of ligand (2 mmol) in 20 cm^3 methanol was added a solution of the metal sulfate or chloride (2 mmol) in methanol (10 cm^3). The reaction mixture was stirred at room temperature for 1 h. The pH of the mixture was then raised to 6.0 by adding 5% aqueous NaOH solution (1 cm^3) dropwise with constant stirring. Stirring was then continued for 4 h. The resulting precipitate was collected by filtration and recrystallized from methanol.

3. Results and discussion

Reactions of the hydrated metal ions $CuSO_4 \cdot 5H_2O$, $CoSO_4 \cdot 7H_2O$, $NiCl_2 \cdot 6H_2O$, $ZnSO_4 \cdot 7H_2O$ and $CdSO_4 \cdot 8/3H_2O$ with Schiff-base ligands L^1–L^8 in a 1 : 1 (M:L) molar ratio gave their corresponding complexes (**1**–**15**), which were confirmed by elemental analysis (table 1). Ligands L^1 and L^5 are tridentate towards the divalent metal ions; L^2, L^4, L^6 and L^8 are neutral tetradentate towards the divalent metal ion; and L^3 and L^7 are dianionic tetradentate towards the metal ions. Chemical analyses (table 1), together with the molar conductance data (Ω m) in DMF (1×10^{-3} M) (2.9–30.6 $ohm^{-1}\,cm^2\,mol^{-1}$), for the complexes indicated their nonionic character, as well as the coordination of SO_4^{2-} or Cl^- ions to the central metal(II) ions [16,17]. Complex **12**, $[NiL^2]Cl_2$, has a molar conductance of 192.5 $ohm^{-1}\,cm^2\,mol^{-1}$, indicating its ionic character. Mass spectral data for complexes **1**–**12**, reported in table 1, show that the parent peak in each of these mass spectra corresponds to the molecular weight of that complex, and indicates the suggested structures of the parent ligands.

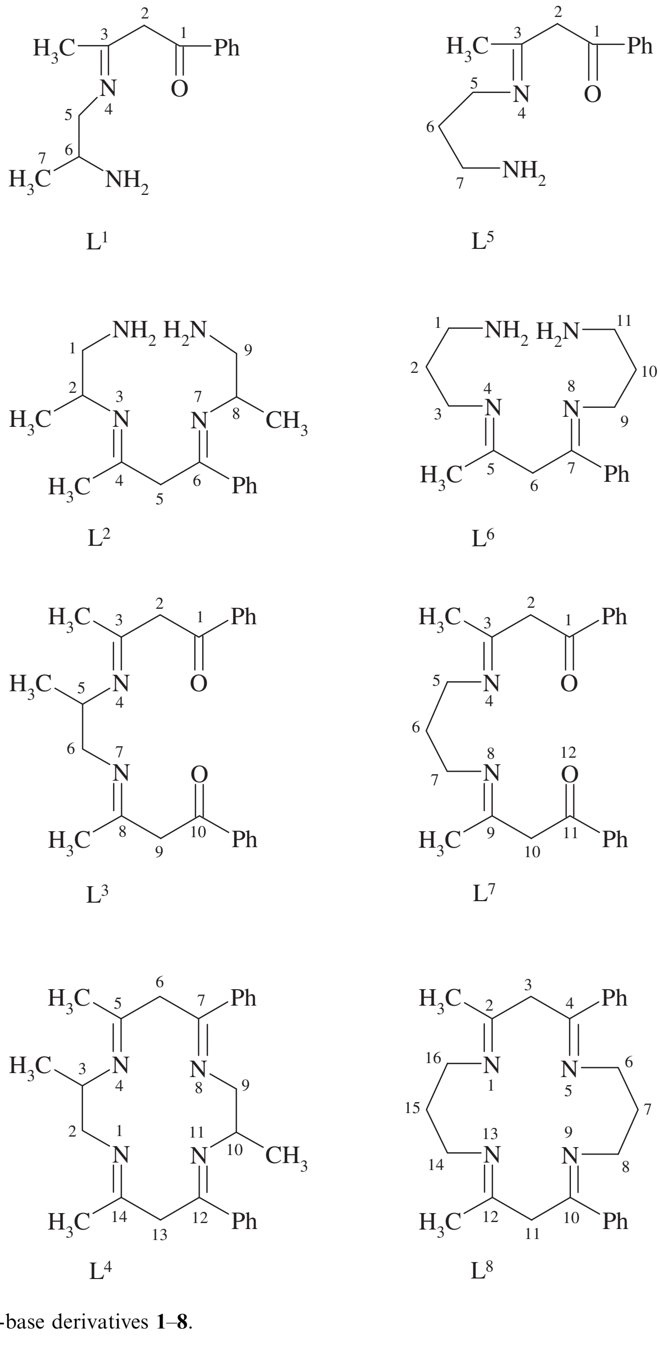

Figure 1. Schiff-base derivatives **1**–**8**.

3.1. *Thermogravimetric analysis*

TGA of the solid complexes indicate a common behavior (table 2). The thermograms can be subdivided into four main regions: the first region extends up to 168°C for

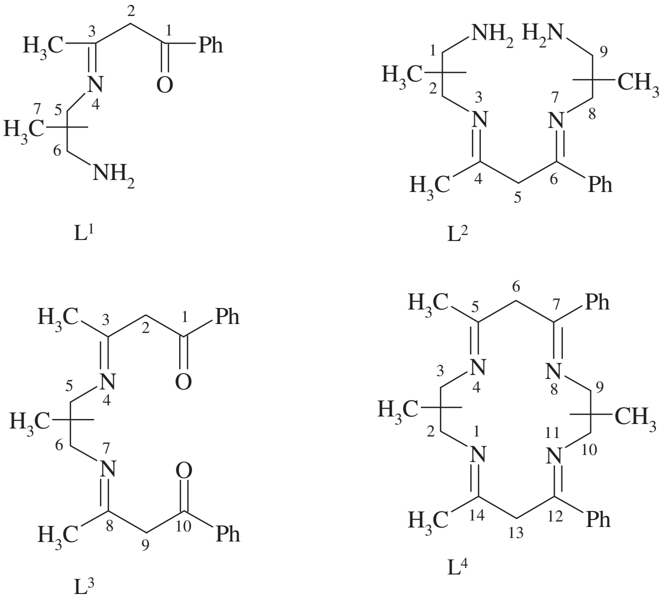

Figure 2. Formulation of L^1–L^4.

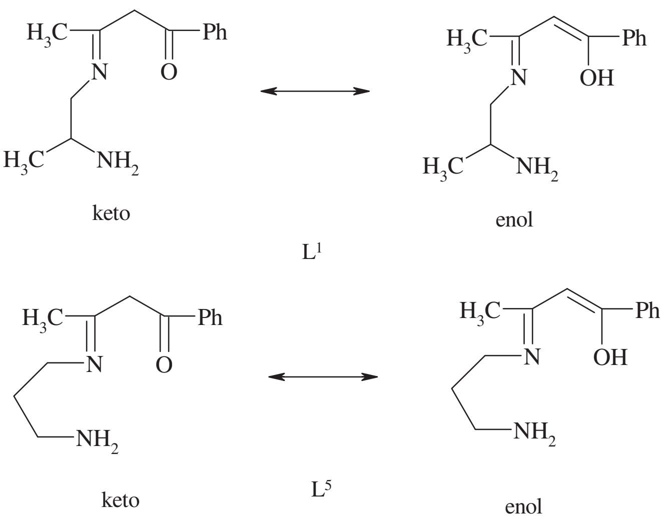

Figure 3. Keto–enol tautomeric forms of L^1 and L^5.

elimination of coordinated water. The second region up to 307°C includes elimination of the coordinated or noncoordinated SO_4^{2-} or Cl^- ions. The third region indicates thermal stability and extends up to 515°C. The fourth region extends up to 800°C and represents decomposition of the complex to the metal oxide. The metal content in the residue was calculated and found to be consistent with the elemental analyses of the complexes.

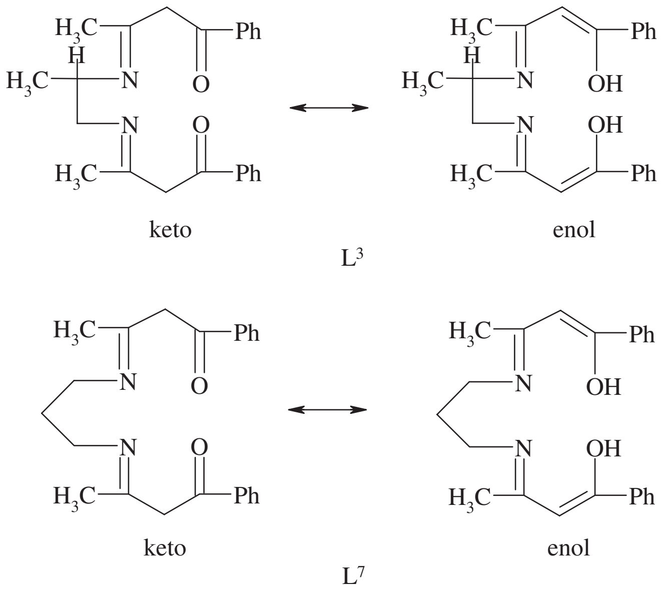

Figure 4. Keto–enol tautomeric forms of L^3 and L^7.

3.2. *IR spectra*

The complexes exhibited strong IR bands (table 3) at 1545–1598 cm^{-1} (C=N), lower than those of the free ligands (1600–1659 cm^{-1}), that is on coordination, $\nu_{C=N}$ shifts to lower a wavenumber. New bands ν_1 (964–997 cm^{-1}) and ν_3 (1208–1249, 1101–1145, 1026–1095 cm^{-1}), which are absent in the spectra of the free ligands, are assigned to coordinated SO_4^{2-} [16,17], and bands in the range 343–362 cm^{-1} are assigned to the coordinated Cl^- ion. New bands in the IR spectra of all metal chelates, which are absent in the IR spectra of the free ligands 336–370 cm^{-1}, are assigned to ν_{M-N}. For Cu complexes of L^3 and L^7, new bands at 475 and 498 cm^{-1} are assigned to ν_{M-O}. In the case of L^3 and L^7, the enolic OH [18] stretching absorption, a broad shallow band 3105–2939 cm^{-1}, disappears on formation of the Ni(II) and Cu(II) complexes of L^3 and the Cu(II) complex of L^7. The Cu complexes of L^2 and L^6 and the Co complex of L^2 display bands at 3422–3441 and 3202–3268 cm^{-1}, respectively, assignable to νNH_2; that is on coordination, the νNH_2 band shifted to lower wavenumber. The Cu(II) complexes of L^1 and L^5 and the Co(II) and Ni(II) complexes of L^1 exhibit a broad band at 3560–3654 cm^{-1} attributed to ν_{OH} of the water molecules associated with complex formation.

3.3. *^{1}H NMR spectra*

The structures of the ligands were confirmed by ^1H NMR measurements. ^1H NMR spectra of ligand **2** gave an H_2N signal at $\delta 2.88$ ppm, which shifted upfield in its diamagnetic complexes [12,14,15] of Ni(II), Zn(II) and Cd(II) to $\delta 2.49$, $\delta 2.56$ and $\delta 2.49$ ppm, respectively, confirming coordination of the NH_2 group. Resonances due to CH_2, CH and CH_3 gave signals at $\delta 3.82$, $\delta 2.28$ and $\delta 2.05$ ppm, respectively, which were

Table 1. Elemental analysis and some physical properties of the solid complexes.

Complex	Color	Yield (%)	Mp (°C)	FW	Analysis found % (calculated %)					Λ (ohm^{-1} cm^{2} mol^{-1})	*m*/*e*
					C	H	N	S	M		
1 [CuL^1(H$_2$O)SO$_4$]	green blue	72	222	394.5	39.3 (39.5)	5.3 (4.8)	7.3 (7.1)	7.8 (8.1)	16.4 (16.1)	18.1	395
2 [CuL^{2}SO$_4$]	violet	81	240	433.5	44.0 (44.3)	6.4 (6.0)	13.2 (12.9)	7.1 (7.4)	15.0 (14.7)	15.8	434
3 [CuL^{3}SO$_4$]	blue green	86	200	519.5	52.7 (53.1)	4.7 (4.6)	5.6 (5.4)	6.4 (6.2)	12.5 (12.2)	30.6	521
4 [CuL^{4}SO$_4$]	green	77	177	559.5	55.6 (55.8)	5.4 (5.7)	9.8 (10.0)	5.4 (5.7)	11.6 (11.4)	30.2	559
5 [CuL^5(H$_2$O)SO$_4$]	blue green	76	194	394.5	39.1 (39.5)	5.1 (4.8)	7.5 (7.1)	7.9 (8.1)	16.3 (16.1)	12.4	395
6 [CuL^{6}SO$_4$]	pale blue	83	175	433.5	44.1 (44.3)	6.3 (6.0)	12.7 (13.0)	7.7 (7.4)	14.5 (14.7)	3.3	433
7 [CuL^{7}SO$_4$]	green gray	88	247	519.5	53.0 (53.1)	4.7 (5.6)	5.7 (5.4)	5.9 (6.1)	12.5 (12.2)	5.9	522
8 [CuL^{8}SO$_4$]	blue gray	84	> 250	559.5	55.6 (55.8)	5.4 (5.7)	9.8 (10.0)	5.5 (5.7)	11.1 (11.4)	4.0	560
9 [CoL^1(H$_2$O)SO$_4$]	light brown	69	223	389.9	39.7 (40.0)	5.2 (4.9)	7.5 (7.2)	7.9 (8.2)	15.0 (15.1)	5.6	391
10 [CoL^{2}SO$_4$]	brown	66	248	428.9	45.1 (44.8)	6.3 (6.1)	12.7 (13.0)	7.6 (7.5)	13.8 (13.7)	2.8	429
11 [NiL^1(H$_2$O)Cl$_2$]	green	73	225	346.6	42.7 (42.8)	5.5 (5.2)	7.8 (7.7)	–	16.4 (16.1)	2.9	365
12 [NiL^2]Cl$_2$	pale yellow	78	236	403.6	47.5 (47.6)	6.2 (6.4)	13.6 (13.9)	–	14.1 (14.5)	192.5	403
13 [NiL^3]	pale brown	81	> 250	418.7	66.2 (65.9)	5.8 (5.7)	6.2 (6.7)	–	14.3 (14.0)	20.2	–
14 [ZnL^{2}SO$_4$]	white	65	> 250	435.4	44.0 (44.1)	6.4 (6.0)	12.6 (12.9)	7.5 (7.3)	14.8 (15.0)	3.8	–
15 [CdL^{2}SO$_4$]	yellow	68	> 250	482.4	39.6 (39.8)	5.1 (5.4)	11.3 (11.6)	6.4 (6.6)	23.5 (23.3)	3.0	–

Table 2. Thermogravimetric analysis of Cu(II), Co(II), Ni(II), Zn(II) and Cd(II) complexes.

Complex	Temp. range (°C)	% Loss calcd (found)		Lost fragments	Residue
1 [CuL^1(H$_2$O)SO$_4$]	128–160	4.56 (4.60)		One coordinated H$_2$O	[CuL^{1}SO$_4$]
	160–220	24.27 (24.00)		A coordinated SO$_4^{2-}$ ion	[CuL^1]
	253–315		Thermal stability		
	450–715	54.99 (54.50)			CuO
2 [CuL^2 SO$_4$]	181–256	22.14 (21.94)		A coordinated SO$_4^{2-}$ ion	[CuL^2]
	261–372		Thermal stability		
	485–800	63.19 (63.41)			CuO
3 [CuL^{3}SO$_4$]	176–235	18.47 (18.37)		A coordinated SO$_4^{2-}$ ion	[CuL^3]
	246–344		Thermal stability		
	434–730	69.28 (69.00)			CuO
4 [CuL^{4}SO$_4$]	183–255	17.16 (17.27)		A coordinated SO$_4^{2-}$ ion	[CuL^4]
	385–490		Thermal stability		
	590–760	71.48 (71.55)			CuO
5 [CuL^5(H$_2$O)SO$_4$]	135–166	4.56 (4.72)		One coordinated H$_2$O	[CuL^{5}SO$_4$]
	251–307	24.27 (24.51)		A coordinated SO$_4^{2-}$ ion	[CuL^5]
	307–373		Thermal stability		
	412–670	55.11 (55.11)			CuO
6 [CuL^{6}SO$_4$]	217–273	22.14 (22.26)		A coordinated SO$_4^{2-}$ ion	[CuL^6]
	287–356		Thermal stability		
	418–742	63.19 (62.96)			CuO
7 [CuL^{7}SO$_4$]	203–268	18.47 (18.63)		A coordinated SO$_4^{2-}$ ion	[CuL^7]
	275–346		Thermal stability		
	453–778	69.28 (69.43)			CuO
8 [CuL^{8}SO$_4$]	185–255	17.16 (16.95)		A coordinated SO$_4^{2-}$ ion	[CuL^8]
	320–385		Thermal stability		
	408–793	71.48 (71.38)			CuO
9 [CoL^1(H$_2$O)SO$_4$]	124–168	4.61 (4.88)		One coordinated H$_2$O	[CoL^{1}SO$_4$]
	183–244	24.55 (24.64)		A coordinated SO$_4^{2-}$ ion	[CoL^1]
	244–309		Thermal stability		
	437–715	55.64 (55.32)			CoO
10 [CoL^{2}SO$_4$]	196–284	22.38(22.18)		A coordinated SO$_4^{2-}$ ion	[CoL^{2}SO$_4$]
	297–364		Thermal stability		
	398–782	63.87 (64.11)			CoO
11 [NiL^1(H$_2$O)Cl$_2$]	125–226	4.93 (4.81)		One coordinated H$_2$O	[NiL^{1}Cl$_2$]
	226–262	19.39 (19.12)		Two coordinated Cl$^-$ ions	[NiL^1]
	305–383		Thermal stability		
	416–762	59.51 (59.92)			NiO
12 [NiL^2]Cl$_2$	233–267	17.56 (17.63)		Two Cl$^-$ ions	[NiL^2]
	415–445		Thermal stability		
	450–795	67.88 (67.72)			NiO
14 [ZnL^{2}SO$_4$]	186–263	22.04 (22.15)		A coordinated SO$_4^{2-}$ ion	[ZnL^2]
	315–492		Thermal stability		
	525–712	62.93 (62.83)			ZnO
15 [CdL^{2}SO$_4$]	192–273	19.90 (20.24)		A coordinated SO$_4^{2-}$ ion	[CdL^2]
	332–515		Thermal stability		
	562–734	56.79 (56.55)			CdO

shifted upfield in the complexes to 3.36–3.70, 2.25–2.15 and 1.98–2.02 ppm, respectively. Aromatic proton signals in the macrocyclic group do not shift upfield [19]. The ^{1}H NMR spectra of L^3 gave a broad signal of the enolic OH proton at 11.5 ppm (keto–enol conversion is slow enough so that the absorption peaks of both forms can be observed), which disappears on complex formation, indicating coordination to the metal through oxygen. The resonances due to CH$_3$, CH$_2$ and CH gave signals at 2.08, 3.52 and 4.02 ppm, respectively, which shifted upfield in complex **13** to 1.83,

Table 3. Important IR spectral bands (cm^{-1}) for selected metal complexes.

Complex	ν_{OH} H_2O	νNH_2	$\nu_{C=N}$ coord	ν_1 S–O	ν_3 S–O	$\nu_{M–N}$	$\nu_{M–O}$	Other bands
1 $[CuL^1(H_2O)SO_4]$	3560	–	1591	964	1208 1115 1067	350	460	–
2 $[CuL^2SO_4]$	–	3424 3246	1593	965	1215 1122 1060	370	456	–
3 $[CuL^3SO_4]$	–	–	1598	984	1210 1145 1093	360	475	–
4 $[CuL^4SO_4]$	–	–	1587 1565	983	1249 1144 1095	343	455	–
5 $[CuL^5(H_2O)SO_4]$	3650	–	1591	988	1211 1144 1094	353	464	–
6 $[CuL^6SO_4]$	–	3341 3268	1594 1559	970	1221 1118 1047	365	459	–
7 $[CuL^7SO_4]$	–	–	1582	982	1210 1117 1046	355	458	–
8 $[CuL^8SO_4]$	–	–	1592 1558	980	1220 1117 1026	349	460	–
9 $[CoL^1(H_2O)SO_4]$	3650	–	1594	966	1243 1101 1061	355	456	–
10 $[CoL^2SO_4]$	–	3422 3202	1593 1558	969	1228 1119 1067	344	466	–
11 $[NiL^1(H_2O)Cl_2]$	3653	–	1596	–	–	336	452	M–Cl 362
12 $[NiL^2]Cl_2$	–	–	1598	–	–	364	–	–
13 $[NiL^3]$	–	–	1595 1564	–	–	354	451	–
14 $[ZnL^2SO_4]$	–	3428	1592 1559	966	1212 1122 1063	348	460	–
15 $[CdL^2SO_4]$	–	3445	1598 1545	997	1240 1122 1070	352	458	–

2.49 and 3.42 ppm, respectively. Upfield shift of these protons supports coordination of Ni(II) to the ligand.

3.4. *Visible spectra of the metal complexes*

Visible spectra of the metal complexes were obtained in DMF and nujol mull (table 4; figures 5–7). Electronic spectra of the Cu(II) complexes showed five main bands with λ_{max} at 247–277, 324–352, 430–567, 618–670 and 733–787 nm in DMF and at 225–255, 315–330, 420–569, 629–685 and 732–765 nm in nujol mull. In both DMF and nujol mull, the first three bands can be assigned to $\pi - \pi^*$ within the aromatic ring, C=N and a charge transfer band (L→Cu), respectively; the bands display small shifts from those of the free ligands as a result of complex formation. The last two bands can be assigned to the electronic transitions $^2Eg \rightarrow ^2T_{2g}$ and $^2B_{1g} \rightarrow ^2B_{2g}$, which are relevant to distorted octahedral geometry around the central Cu(II) ion [20,21]. Therefore, it may be concluded that all the complexes formed by macrocycles with Cu(II) metals are distorted octahedral. This is further supported by the magnetic moment values (1.65–2.2 BM) (table 4), within the required range for d^9 systems [22]. Electronic spectra of the Co(II) complexes of L^1 and L^2 also showed five bands with λ_{max} at 228–274, 350–316, 450–550, 650–675 and 703–708 nm in DMF and 225–245, 320–330, 464–505, 663–682 and 710–716 nm in nujol mull. In both DMF and nujol mull, the first three bands can be assigned to $\pi - \pi^*$ within the aromatic ring, C=N and a charge transfer band (L→Co), respectively. The last two bands can be assigned to $^4T_{1g(F)} \rightarrow ^4T_{1g(P)}$ and $^4T_{1g(F)} \rightarrow 4A_{2g}$ transitions, respectively, indicating octahedral

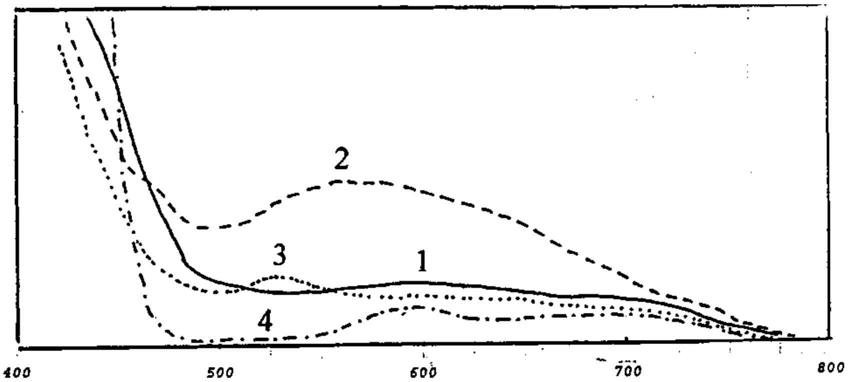

Figure 5. Reflectance spectra of Cu(II) complexes **1**–**4**.

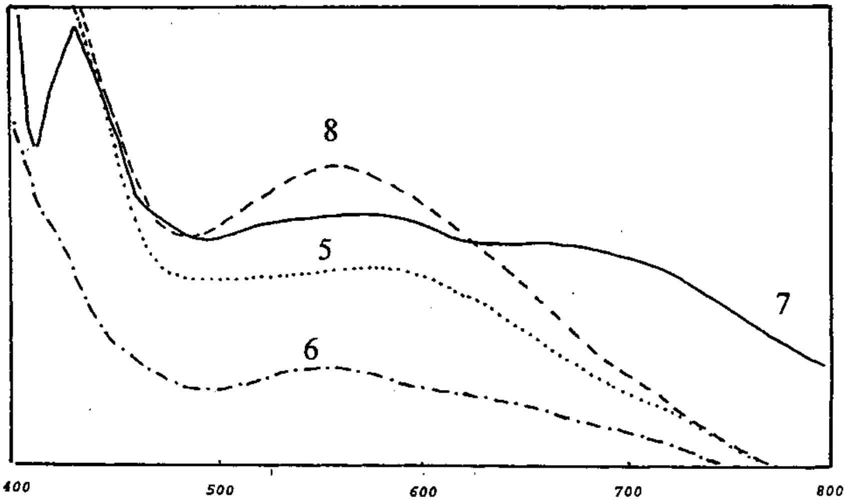

Figure 6. Reflectance spectra of Cu(II) complexes **5**–**8**.

geometry [23]. The effective magnetic moment values (4.84–4.51 BM) are within the range expected for octahedral Co(II) complexes [24]. Electronic spectra of Ni(II) complexes of L^1 exhibit five bands with λ_{max} at 260, 340, 428, 623 and 658 nm in DMF and 244, 332, 419, 630 and 663 nm in nujol mull. The first three bands can be assigned to $\pi - \pi^*$ within the aromatic ring, C=N and a charge transfer band (L→Ni), respectively, with small shifts from those of the free ligands as a result of complex formation. The last two bands are due to $^3A_{2g} \rightarrow {}^3T_{1g(F)}$ transition in an octahedral field. The appearance of a doublet for this transition may be ascribed to gain of intensity of the $^3A_{2g} \rightarrow {}^1E_g$ transition through configurational interaction with the $^3T_{1g(F)}$ level [25] and also to spin–orbit coupling [26]. The transition $^3A_{2g} \rightarrow {}^3T_{1g(P)}$ is obscured by the charge transfer bands. The Ni(II) complexes of ligands L^2 and L^3 are pale yellow and pale brown, respectively. Their electronic spectra show absorption bands

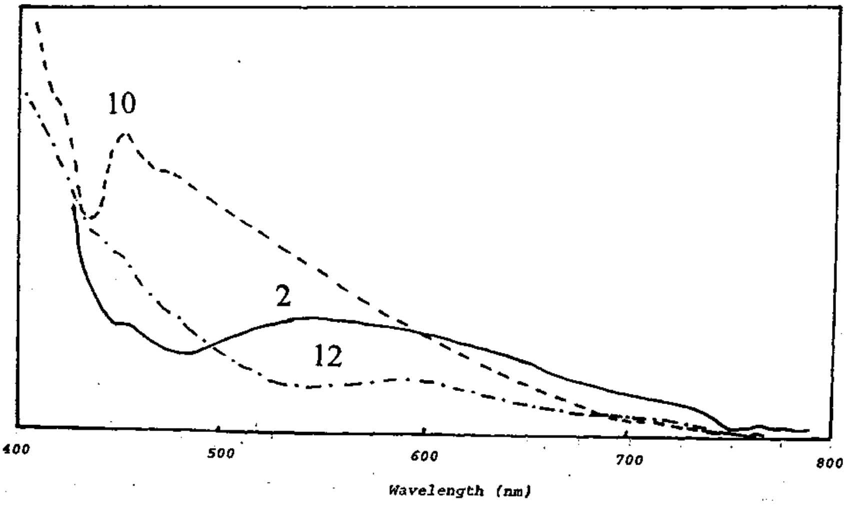

Figure 7. Reflectance spectra of Cu(II), Co(II) and Ni(II) complexes of ligand L^2 (complexes **2**, **10** and **12**).

with λ_{max} at (227, 336, 548, 587), (220, 330, 548, 590) nm for L^2 in DMF and nujol mull, respectively, and λ_{max} at (239, 352, 550, 610), (242, 353, 536, 600) nm for the Ni(II) complex of L^3 in DMF and nujol mull, respectively. These bands are presumed to be $\pi-\pi^*$ of the aromatic ring, C=N, charge transfer and ${}^1A_{1g} \rightarrow {}^1A_{2g}$ transitions. The latter band indicates the square-planar configuration of the complexes [27]. Although zinc has a greater preference for tetrahedral $M[N_4]$ coordination, found for tetrahedral template molding structures of many enzymes [28,29], the Zn(II) and Cd(II) complexes are six-coordinate [30,31] as indicated by elemental analysis and spectral data, which confirm the octahedral structure. The Zn(II) and Cd(II) complexes are diamagnetic, as expected for a d^{10} system.

4. Conclusion

Based on the above results, the structures of the complexes under investigation can be formulated as shown in figures 8–14.

4.1. *Antimicrobial screening*

Agar disk diffusion was used to test antifungal activity [14,32]. The organisms were tested against the activity of different concentrations of the ligands and complexes, and the results are shown in table 5.

The test was carried out on the surface of Czapeck's agar medium seeded with *Aspergillus fumigatus*, *Penicillium italicum*, *Syncephalastrum racemosum* and *Candida albicans* at 30°C and incubated for 3 days; the average diameter of the inhibition zone was recorded for each compound. The ligands and complexes showed positive

Table 4. Visible spectral values for Cu(II), Co(II), Ni(II), Zn(II) and Cd(II) complexes of Schiff bases in DMF and nujol mull, respectively, and their magnetic moments.

		Band assignment						
		λ_{max} (nm)			d–d transition (λ_{max} nm)			
Complex	Color	$\pi-\pi^*$ aromatic ring	$\pi-\pi^*$ C=O	$\pi-\pi^*$ C=N	CT L→Cu	$^2E_g \rightarrow {}^2T_{2g}$	$^2B_{1g} \rightarrow {}^2B_{2g}$	Magnetic moment (BM)
1 [CuL^1(H$_2$O)SO$_4$]	green	277	–	352	430	618	787	1.65
	blue	230		315	420	629	765	
2 [CuL^{2}SO$_4$]	violet	252	–	348	540	670	762	2.13
		236		330	554	685	755	
3 [CuL^{3}SO$_4$]	blue	276	–	350	550	637	753	2.2
	green	255		317	550	677	744	
4 [CuL^{4}SO$_4$]	green	276	–	348	545	627	770	2.2
		225		317	530	647	748	
5 [CuL^5(H$_2$O)SO$_4$]	blue	276	–	352	571	620	764	1.73
	green	228		325	569	635	732	
6 [CuL^{6}SO$_4$]	pale	275	–	324	562	618	733	1.67
	blue	240		318	572	650	750	
7 [CuL^{7}SO$_4$]	green	247	–	352	552	627	747	1.81
	gray	229		313	554	670	741	
8 [CuL^{8}SO$_4$]	blue	276	–	349	567	650	758	1.75
	gray	230		328	553	680	752	
					CT L→Co	$^4T_{1g(F)} \rightarrow {}^4T_{1g(P)}$	$^4T_{1g(F)} \rightarrow {}^4A_{2g}$	
9 [CoL^1(H$_2$O)SO$_4$]	light	274	–	316	550	650	708	4.51
	brown	245		330	505	663	710	
10 [CoL^{2}SO$_4$]	brown	228	–	350	450	675	703	4.84
		225		320	464	682	716	
					CT L→Ni	$^3A_{2g} \rightarrow {}^3T_{1g(F)}$		
11 [NiL^1(H$_2$O)Cl$_2$]	green	260	–	340	428	623 658	–	3.42
		244		332	419	630 663		
					CT L→Ni	$^1A_{1g} \rightarrow {}^1A_{2g}$		
12 [NiL^2]Cl$_2$	pale	227	–	336	548	587	–	–
	yellow	220		330	548	590		
13 [NiL^3]	pale	239	–	352	550	610	–	–
	brown	242		353	536	600		
					CT L→Zn or Cd			
14 [ZnL^{2}SO$_4$]	white	228	–	352	480	–	–	–
		233		330	494			
15 [CdL^{2}SO$_4$]	yellow	230	–	354	507	–	–	–
		249		334	581			

and negative inhibition values (table 5). The metal complexes were found to be more active in all cases than their corresponding ligands, confirming that chelation of metal to ligand increases the toxicity of the compound [14,32]. The growth inhibition capacity follows the order sulfato complexes > chloro complexes > ligands, and we conclude that the sulfate ion is responsible for the growth of the inhibition capacity of the complexes.

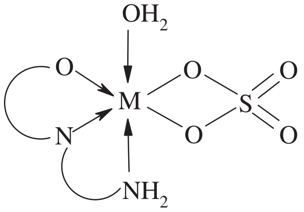

Figure 8. Octahedral structures of metal complexes of ligands L^1 and L^5, M = Cu(II) and Co(II) (complexes **1**, **5** and **9**).

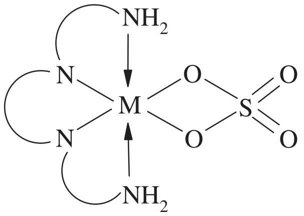

Figure 9. Octahedral structures of metal complexes of ligands L^2 and L^6, M = Cu(II) and Co(II), Zn(II) and Cd(II) (complexes **2**, **6**, **10**, **14** and **15**).

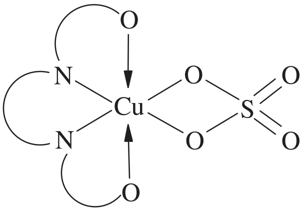

Figure 10. Octahedral structures of Cu(II) complexes of ligands L^3 and L^7 (complexes **3** and **7**).

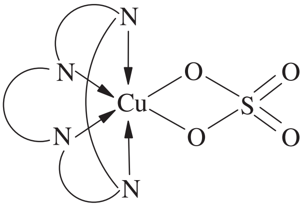

Figure 11. Octahedral structures of Cu(II) complexes of ligands L^4 and L^8 (complexes **4** and **8**).

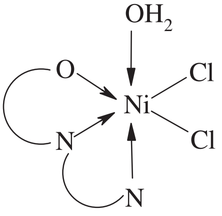

Figure 12. Octahedral structure of Ni(II) complex of ligand L^1 (complex **11**).

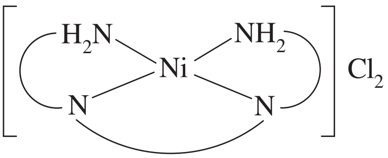

Figure 13. Square-planar structure of Ni(II) complex of ligand L^2 (complex **12**).

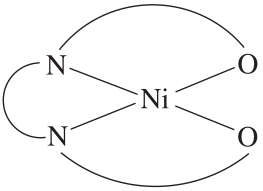

Figure 14. Square-planar structure of Ni(II) complex of ligand L^3 (complex **13**).

Table 5. Antifungal activity of the ligands and their complexes at concentrations of 5, 2.5 and 1 mg ml^{-1}.

	Aspergillus fumigatus			*Penicillium italicum*			*Syncephalastrum racemosum*			*Candida albicans*		
	5	2.5	1	5	2.5	1	5	2.5	1	5	2.5	1
L^1	+	+	+	+	+	+	+	−	−	+	−	−
1 $[\mathrm{CuL^1(H_2O)SO_4}]$	++	++	+	++	++	++	+	+	−	+	+	+
9 $[\mathrm{CoL^1(H_2O)SO_4}]$	++	++	+	++	+	+	+	+	−	+	+	−
11 $[\mathrm{NiL^1(H_2O)SO_4}]$	++	++	+	++	+	+	++	+	−	++	+	−
L^2	+	+	−	+	+	+	+	−	−	+	+	−
2 $[\mathrm{CuL^2SO_4}]$	++	++	+	++	+	+	++	+	+	++	++	++
10 $[\mathrm{CoL^2SO_4}]$	++	+	+	++	+	+	++	+	−	++	++	++
12 $[\mathrm{NiL^2}]\mathrm{Cl_2}$	+	+	+	+	−	−	+	−	−	++	++	++
14 $[\mathrm{ZnL^2SO_4}]$	++	++	+	++	++	+	++	+	−	++	++	++
15 $[\mathrm{CdL^2SO_4}]$	++	++	+	++	++	+	++	+	−	++	++	++
L^3	+	+	−	+	−	−	+	+	+	+	+	+
3 $[\mathrm{CuL^3SO_4}]$	++	++	+	++	+	+	+	−	−	++	+	+
13 $[\mathrm{NiL^3}]$	+	+	+	++	++	++	+	+	+	+	+	+
L^4	+	+	+	+	+	−	+	+	−	+	+	+
4 $[\mathrm{CuL^4SO_4}]$	++	++	+	++	++	++	++	++	−	++	++	++
L^5	+	+	+	+	+	+	+	+	+	+	+	+
5 $[\mathrm{CuL^5(H_2O_2)SO_4}]$	++	++	++	++	++	++	++	+	+	++	++	++
L^6	+	+	−	+	+	+	−	−	−	+	+	−
6 $[\mathrm{CuL^6SO_4}]$	++	++	++	++	+	−	+	+	+	++	++	++
L^7	+	+	+	+	+	−	−	−	−	+	+	+
7 $[\mathrm{CuL^7SO_4}]$	++	++	++	++	+	+	+	+	+	++	++	++
L^8	++	+	+	+	+	−	+	+	+	+	+	+
8 $[\mathrm{CuL^8SO_4}]$	++	++	++	++	++	+	+	+	+	++	++	++
St	+++	+++	++	+++	+++	++	+++	+++	+++	++	++	++

St = reference standard; terbinafin was used as a standard antifungal agent.
Well diameter = 0.6 cm (100 µl of each concentration was tested).
Inhibitions values: +, 0.1–0.5 cm beyond control; ++, 0.6–1.0 cm beyond control; +++, 1.1–1.5 cm beyond control; –, not detected.
Solvent = DMF.

References

[1] K. Kumar, M.F. Twiddle, *Pure Appl. Chem.* **65**, 512 (1993).
[2] F.H. Fry, B. Graham, L. Spicca, D.C.R. Hockles, E.R.T. Tiekink, *J. Chem. Soc., Dalton Trans.* 827 (1997).
[3] M. Rosignoli, P.V. Bernhardt, G.A. Lawrence, M. Maeder, *J. Chem. Soc., Dalton Trans.* 323 (1997).
[4] X. Xu, Q. Luo, M. Shen, X. Huang, Q. Wu, *Polyhedron* **16**, 915 (1997).
[5] A.J. Blake, I.A. Fallis, R.O. Gould, S. Parsons, S.A. Ross, M. Schroder, *J. Chem. Soc., Dalton Trans.* 4379 (1996).
[6] M.F. Huzenkamp, A.C. Stucke, E. Cavoli, H.U. Gudel, *J. Chem. Soc., Dalton Trans.* 251 (2000).
[7] A. Levine, P.A. Lay, N.F. Dixon, *Inorg. Chem.* **39**, 385 (2000).
[8] S. Belviso, G. Ricciardi, F. Lelj, L.M. Scolaro, A. Bencini, C. Carbonera, *J. Chem. Soc., Dalton Trans.* 1143 (2001).
[9] S. Chardra, S.D. Sharma, *J. Indian Chem. Soc.* **79**, 495 (2002).
[10] D. Esteban, D. Bânobre, R. Bastida, A. de Blas, A. Maciás, A. Rodŕiguez, T. Rodriguez Blas, D.E. Fenton, H. Adams, J. Mahia, *Inorg. Chem.* **38**, 1937 (1999).
[11] H. Masuda, T. Sugimari, T. Kohzuma, A. Odani, O. Yamauchi, *Bull. Chem. Soc. Jpn.* **65**, 789 (1992).
[12] M.A. Halcrow, G. Christou, *Chem. Rev.* **94**, 2421 (1994).
[13] A.A. Saleh, B. Pleune, J.C. Fettinger, R. Poli, *Polyhedron* **16**, 1391 (1997).
[14] A.A. Saleh, S.M.E. Khalel, M.F. Eid, M.A. El-Ghamry, *J. Coord. Chem.* **56**, 467 (2003).
[15] (a) A.L. Nivorozhkin, H. Toftlund, P.L. Jorgensen, L.E. Nivorozhkin, *J. Chem. Soc., Dalton Trans.* 1215 (1996); (b) H. Adams, R.M. Bucknall, D.E. Fenton, C.O. Rodriguez de Barbarin, M. Garcia, J. Oakes, *Polyhedron* **17**, 3803 (1998); (c) S. Ranganathan, N. Tamilarasu. *Inorg. Chem.* **38**, 1019 (1999); (d) J.P. Costes, J.M. Dominguez-Vera, J.P. Laurent, *Polyhedron* **14**, 2179 (1995).
[16] (a) K. Nakamoto, *Infrared and Raman Spectra of Inorganic and Coordination Compounds*, 4th edn, Wiley-Interscience, New York (1986); (b) J.W. Geary, *Coord. Chem. Rev.* **7**, 81 (1971).
[17] A.A. Saleh, F.M. El-Zawawy, S.M. Abu El-Wafa, *Egypt. J. Chem.* **36**, 373 (1993).
[18] R.M. Silverstein, G.C. Bassler, T.C. Morrill, *Spectrometric Identification of Organic Compounds*, 4th edn. (1981).
[19] R. Singh, A. Bhattacharya, P. Kumar, *J. Indian Chem. Soc.* **79**, 525 (2002).
[20] M.J.M. Campbell, R. Grezeskoviak, *Inorg. Nucl. Chem. Lett.* **5**, 27(1969).
[21] A.B.P. Lever, *Inorganic Electronic Spectroscopy*, 2nd edn (1997).
[22] J. Lewis, R.G. Wilkins, *Modern Coordination Chemistry*, Interscience, New York (1967).
[23] R.K. Parihari, R.K. Patel, R.N. Patel, *J. Indian Chem. Soc.* **77**, 339 (2000).
[24] B.N. Figgis, *Introduction to Ligand Field*, Wiley Eastern, New Delhi, (1976).
[25] (a) C.K. Jorgensen, *Acta Chem. Scand.* **9**, 1362 (1955); (b) O.G. Holmes, D.S. McClure, *J. Chem. Phys.* **26**, 1686 (1957).
[26] A.D. Liehr, C.J. Ballhausen, *Ann. Phys.* 6; *Mal. Phys.* **2**, 123 (1959).
[27] J.C. Bailar, H.J. Emeléus, R. Nyholm, A.F. Trotman-Dickenson, *Comprehensive Inorganic Chemistry*, Pergamon Press, (1975).
[28] R. Han, A. Looney, K. McNeil, G. Parkin, A.L. Rheirgold, B.S. Haggerty, *J. Inorg. Biochem.* **49**, 105 (1993).
[29] A. Looney, A. Saleh, Y. Zhang, G. Parkin, *Inorg. Chem.* **33**, 6 (1994).
[30] N.N. Greenwood, A. Earnshaw, *Chemistry of the Elements* (1989).
[31] K.H. Reddy, P.S. Reddy, *J. Indian Chem. Soc.* **79**, 132 (2002).
[32] Y. Bodke, S.S. Sangapure, *J. Indian Chem. Soc.* **80**, 187 (2003).